ANALYSIS OF AN ENERGY LOCALIZATION APPROXIMATION APPLIED TO THREE-DIMENSIONAL KINETIC MONTE CARLO SIMULATIONS OF HETEROEPITAXIAL GROWTH

KYLE L. GOLENBIEWSKI[†] AND TIM P. SCHULZE[†]

Abstract. Heteroepitaxial growth involves depositing one material onto another with a different lattice spacing. This misfit leads to long-range elastic stresses that affect the behavior of the film. Previously, an Energy Localization Approximation was applied to Kinetic Monte Carlo simulations of two-dimensional growth in which the elastic field is updated using a sequence of nested domains. We extend the analysis of this earlier work to a three-dimensional setting and show that while it scales with the increase in dimensionality, a more intuitive Energy Truncation Approximation does not.

Key words. kinetic Monte Carlo, heteroepitaxy, elasticity

1. Introduction. This paper concerns heteroepitaxial thin films—thin layers of crystalline material that have been deposited on a crystalline substrate. Such films are used in a wide variety of applications, including the fabrication of semiconductors, which has lead to the production of high-brightness light-emitting diodes, lasers, and high-frequency transistors [2]. Since the two species will typically have a lattice mismatch, the behavior of the film is heavily influenced by long-range elastic stresses ([1],[4]).

At the atomistic level, Kinetic Monte Carlo (KMC) is an effective way of simulating the growth and evolution of such films ([6]-[11]). KMC simulates both a crystal's evolution toward equilibrium and the influence of nonequilibrium processes, such as deposition. It does this via a Markov Chain model, where potential configuration changes are assigned rates. The rates themselves can be deduced from experiments, calculated from energy landscape calculations and transition state theory, or given by empirical models. When elastic forces are absent, a typical model is to assume single-atom moves to neighboring lattice sites with a rate that scales exponentially with the number of nearest neighbors. For an atom i, this rate is

$$r_i = ke^{-(\gamma n_i)/k_bT},$$

where n_i is the total number of nearest neighbor bonds with atom i, γ is the bond energy, k_bT is the thermal energy, and k is a scaling factor. While far from the most accurate approach, these "bond counting" models offer heuristic insight into a system's behavior while being significantly faster and easier

[†]Department of Mathematics, University of Tennessee, Knoxville, TN 37996-1320

to implement than more fundamental approaches. The introduction of elastic interactions into these models substantially increases the complexity of KMC, however, and until recently it was not possible to do three-dimensional simulations on practical length and time scales. One of the key ideas that made these simulations possible was the use of an Energy Localization Approximation. This paper is specifically concerned with characterizing the accuracy of this approximation, extending the work of Schulze and Smereka [9] to a three-dimensional setting.

The model that is used for the rates in the particular KMC simulations just mentioned is a hybrid model that combines a nearest-, next-nearest, and third-nearest neighbor bond-counting scheme with an elastic model based on a network of springs obeying Hooke's law. In terms of the hopping rate, this amounts to an additional term, ΔW, that measures the elastic contribution to the energy barrier when atom i hops:

$$r_i = ke^{-(\gamma n_i + \Delta W)/k_b T)}.$$

The elastic contribution to the energy barrier is modeled as the difference in the total elastic energy with and without the atom for which the rate is being calculated. If one were to fully implement this model, it would involve a prohibitively high computational complexity. The essence of the Energy Localization Approximation is to do a local calculation centered on the atom in question. Intuitively, it seems that this might be promising, as we are only changing the network of interacting springs at a single lattice site. Nevertheless, elastic forces are notoriously long-ranged, with Green's tensors that decay like one over distance. So it is somewhat surprising that the accuracy of this method turns out to scale significantly better than this. This is due to a fortunate cancellation of boundary terms in what would otherwise be the largest contributor to the error. This assessment is made by analyzing the analogous problem in the context of linear elasticity.

2. Analysis of Energy Localization in a Three-Dimensional Setting. For the theorems that follow, we consider a system in which a substrate occupying the entire half-space $z < 0$ is completely covered by a small-amplitude film $0 \leq z \leq h(x, y)$ of uniform height H for $x^2 + y^2 > R^2$ (see Figure 1 in Section 2.1). The displacement of the film, $\mathbf{u}$, is measured relative to a reference configuration where a flat film sitting atop the substrate is in mechanical equilibrium. With this choice, it can be shown that the vertical

lattice spacing, a_L, of the film in equilibrium is

$$a_L = a_f + a_s \alpha_1 \frac{2\lambda}{\lambda + 2\mu}, \tag{1}$$

where a_f is the natural lattice spacing of the film, a_s is the lattice spacing of the substrate, α_1 is the scaled misfit given below, and λ and μ are the Lamé constants [8].

Appealing to linear elasticity theory, the elastic energy density of an isotropic material is given by

$$w = \frac{1}{2}\left(\lambda + \frac{2}{3}\mu\right)\left(\sum_{k=1}^{3} E_{kk}\right)^2 + \mu \sum_{i,j=1}^{3}\left(E_{ij} - \frac{1}{3}\delta_{ij}\sum_{k=1}^{3} E_{kk}\right)^2,$$

where $\mathbf{E}$ is the strain tensor defined as the difference[1] of a relative strain $\widetilde{\mathbf{E}}$ and an intrinsic, or stress-free, strain $\overline{\mathbf{E}}$ [3]. Here, we have

$$E_{ij} = \widetilde{E}_{ij} - \overline{E}_{ij},$$

where

$$\widetilde{E}_{ij} = \frac{1}{2}(\partial_i u_j + \partial_j u_i), \quad \text{and} \quad \overline{\mathbf{E}} = \begin{pmatrix} \alpha_1 & 0 & 0 \\ 0 & \alpha_1 & 0 \\ 0 & 0 & \alpha_2 \end{pmatrix} \theta(z);$$

and we use the strain parameters

$$\alpha_1 = \frac{a_f - a_s}{a_s} \quad \text{and} \quad \alpha_2 = \frac{a_f - a_L}{a_s},$$

and the Heaviside function

$$\theta(z) = \begin{cases} 0 & \text{if } z < 0, \\ 1 & \text{if } z > 0. \end{cases}$$

[1]It is noted to the reader that the authors have modified the convention from [9], in which the strain tensor was defined as the sum of a relative and intrinsic strain, to adhere to the more traditional convention in [3]. Likewise for the stress tensor.

Then, expanded out, the energy density is

$$\begin{aligned} w &= \left(\frac{\lambda}{2}+\mu\right)\left[(\partial_1 u_1)^2+(\partial_2 u_2)^2+(\partial_3 u_3)^2\right]+\lambda\left[(\partial_1 u_1)(\partial_2 u_2)+(\partial_1 u_1)(\partial_3 u_3)+(\partial_2 u_2)(\partial_3 u_3)\right] \\ &+\frac{\mu}{2}\left[(\partial_1 u_2)^2+(\partial_2 u_1)^2+(\partial_1 u_3)^2+(\partial_3 u_1)^2+(\partial_2 u_3)^2+(\partial_3 u_2)^2\right] \\ &+\mu\left[(\partial_1 u_2)(\partial_2 u_1)+(\partial_1 u_3)(\partial_3 u_1)+(\partial_2 u_3)(\partial_3 u_2)\right] \\ &-\lambda\left(2\alpha_1+\alpha_2\right)\left[\partial_1 u_1+\partial_2 u_2+\partial_3 u_3\right]\theta(z)-2\mu\left[\alpha_1(\partial_1 u_1+\partial_2 u_2)+\alpha_2\partial_3 u_3\right]\theta(z) \\ &+\left[\frac{\lambda}{2}(2\alpha_1+\alpha_2)^2+\mu(2\alpha_1^2+\alpha_2^2)\right]\theta(z). \end{aligned}$$

We note that the stress tensor, $\mathbf{T}$, is defined through

$$T_{ij}=\frac{\partial w}{\partial_j u_i}.$$

Like the strain tensor, the stress tensor can be written as the difference of a relative stress $\widetilde{\mathbf{T}}$ and an intrinsic stress $\overline{\mathbf{T}}$. Namely,

$$T_{ij}=\widetilde{T}_{ij}-\overline{T}_{ij},$$

where

$$\widetilde{T}_{ij}=2\mu\widetilde{E}_{ij}+\lambda\delta_{ij}\widetilde{E}_{kk} \tag{2}$$

and

$$\overline{\mathbf{T}}=\begin{pmatrix}\sigma_1 & 0 & 0\\ 0 & \sigma_1 & 0\\ 0 & 0 & \sigma_2\end{pmatrix}\theta(z), \tag{3}$$

$$\begin{aligned}\sigma_1 &= 2\left(\lambda+\mu\right)\alpha_1+\lambda\alpha_2, \\ \sigma_2 &= \left(\lambda+2\mu\right)\alpha_2+2\lambda\alpha_1. \end{aligned} \tag{4}$$

The energy density can then be written as

$$\begin{aligned} w &= \sum_{i,j=1}^{3}\left[\frac{\mu}{2}(\partial_i u_j)(\partial_i u_j+\partial_j u_i)+\frac{\lambda}{2}(\partial_i u_i)(\partial_j u_j)-\overline{T}_{ij}\partial_i u_j\right] \\ &+\left[\alpha_1\sigma_1+\frac{\alpha_2}{2}\sigma_2\right]\theta(z). \end{aligned} \tag{5}$$

Noting that

$$T_{ij}=2\mu E_{ij}+\lambda\delta_{ij}E_{kk},$$

the energy density can be compactly written as

$$w = \frac{1}{2}\sum_{i,j=1}^{3} E_{ij}T_{ij}.$$

The equations of equilibrium maintain that for $i \in \{1,2,3\}$,

$$\sum_{j=1}^{3} \partial_j T_{ij} = 0 \quad \text{for } \mathbf{x} \in \Omega,$$

$$\sum_{j=1}^{3} T_{ij} n_j = 0 \quad \text{for } \mathbf{x} \in \partial\Omega.$$

As Schulze and Smereka [9] originally pointed out, the film/substrate interface may introduce a singularity in the first equation due to the stress-free strain. However, it follows from (4), the strain parameters, and (1) that $\sigma_2 = 0$. Written more conveniently in vector notation, we then obtain

$$\mu\Delta\mathbf{u} + (\lambda+\mu)\nabla(\nabla\cdot\mathbf{u}) = \mathbf{0} \quad \text{for } \mathbf{x} \in \Omega, \tag{6}$$

$$\widetilde{\mathbf{T}}\mathbf{n} = \overline{\mathbf{T}}\mathbf{n} \quad \text{for } \mathbf{x} \in \partial\Omega, \tag{7}$$

$$\mathbf{u} \to \mathbf{0} \quad \text{as } |\mathbf{x}| \to \infty. \tag{8}$$

2.1. Energy Localization Approximation. We recall that in Schulze and Smereka [9], the focus was on the ability to efficiently approximate the elastic correction to the energy barrier, denoted ΔW, when transitioning from one state to another. Their model (adopted from [6]) for this was

$$\Delta W = W(\text{with atom } i) - W(\text{without atom } i),$$

where W is the total elastic energy stored in the configuration. Here, we extend their results by showing that the Energy Localization Approximation scales with the increase in dimension. While the model is applied to discrete simulations in practice, the utility of this approximation is shown using the continuum limit of the discrete model.

The total elastic energy stored in an arbitrary configuration is the integral of the energy density over the domain. Namely, for a displacement field $\mathbf{u}$ satisfying (6)-(8),

$$W(\mathbf{u};\Omega) = \int_\Omega w\, d\mathbf{x}. \tag{9}$$

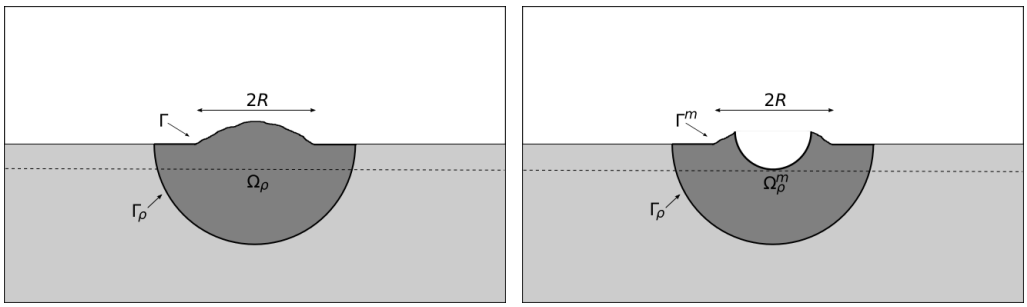

(a) Original Domain (b) Modified Domain

Figure 1. (a) Cross section of the union of the film and substrate (gray), with the truncated domain highlighted in a darker shade of gray. (b) Cross section after the removal of a chunk of material meant to characterize removing an atom in the continuum analogue.

In practice, this is not feasible to calculate. Rather, we consider approximations to the total elastic energy over finite regions $\Omega_\rho \subset \Omega$. Let $\Omega_\rho = \{\Omega \cap \{|\mathbf{x}| < \rho\}\}$. Then, the elastic correction over an unbounded domain is

$$\Delta W = \lim_{\rho\to\infty} \left[W(\mathbf{u};\Omega_\rho) - W(\mathbf{u}^m;\Omega_\rho^m)\right], \tag{10}$$

where Ω_ρ^m is the same domain except that it has been modified locally and $\mathbf{u}^m$ is the corresponding displacement field (see Figure 1). We remind the reader that while the KMC simulations are carried out on a discrete lattice, we consider the continuum analogue for the theorems that follow.

For the Energy Localization Approximation, we constrain the solution on the modified domain to agree with the solution on the original domain along the boundary of the truncated domain below the surface. Namely,

$$\mathbf{u}_\rho^m = \mathbf{u} \quad \text{for } \mathbf{x} \in \Gamma_\rho.$$

Then, the approximation to the displacement field on the modified domain is

$$\mathbf{u}_\rho^m = \begin{cases} \mathbf{u}_\rho^m & \text{if } |\mathbf{x}| < \rho, \\ \mathbf{u} & \text{if } |\mathbf{x}| = \rho. \end{cases}$$

The corresponding Energy Localization Approximation to the elastic correction to the energy barrier is

$$\Delta W_L = W(\mathbf{u};\Omega_\rho) - W(\mathbf{u}_\rho^m;\Omega_\rho^m), \tag{11}$$

which leads us to our first theorem.

THEOREM 1 - Energy Localization Approximation. *Suppose that $h(x, y)$ is a compactly supported function whose support includes $(0, 0)$. Further, suppose that $h(x, y)$ is modified by a localized change centered at $(0, 0)$. Then,*

$$\Delta W - \Delta W_L = O(\epsilon/\rho^3) \quad as \quad \rho \to \infty,$$

where ΔW and ΔW_L are defined by (10) and (11) respectively.

As we see, the error scales by an additional factor of $1/\rho$ when compared to the original two-dimensional result. To gain more appreciation for the Energy Localization Approximation, Schulze and Smereka compared this result with that of an Energy Truncation Approximation. For the truncated approximation, they integrated the *exact* displacement field on the modified domain over the same truncated domain. Then, the Energy Truncation Approximation to the elastic correction to the energy barrier is

$$\Delta W_T = W(\mathbf{u}; \Omega_\rho) - W(\mathbf{u}^m; \Omega_\rho^m). \tag{12}$$

While this may intuitively seem like a better approximation, they showed that this was not the case. Furthermore, in contrast to Theorem 1, the result for the Energy Truncation Approximation does not scale with dimension. Namely,

THEOREM 2 - Nonlocality of the Energy Density. *Under the same hypotheses of Theorem 1,*

$$\Delta W - \Delta W_T = O(\epsilon H/\rho) \quad as \quad \rho \to \infty,$$

where ΔW and ΔW_T are defined by (10) and (12) respectively.

This result further demonstrates the utility of the Energy Localization Approximation as a means of computing the elastic correction to the energy barrier.

2.2. Proof of Theorems. Let $\mathbf{u}$ be a displacement field satisfying (6)-(8). We begin by noting that (5) can be written in vector notation as

$$w = \mu \left(\nabla \cdot \widetilde{\mathbf{E}}\mathbf{u} - \mathbf{u} \cdot \left(\nabla \cdot \widetilde{\mathbf{E}} \right) \right) + \frac{\lambda}{2} (\nabla \cdot \mathbf{u})^2 - \nabla \cdot \overline{\mathbf{T}}\mathbf{u} + \alpha_1 \sigma_1 \theta(z).$$

Furthermore,

$$\nabla \cdot \widetilde{\mathbf{E}} = \frac{1}{2}\left(\Delta \mathbf{u} + \nabla(\nabla \cdot \mathbf{u})\right)$$

and

$$(\nabla \cdot \mathbf{u})^2 = \nabla \cdot (\nabla \cdot \mathbf{u})\mathbf{u} - \mathbf{u} \cdot \nabla(\nabla \cdot \mathbf{u}).$$

Then, recalling (2) and (6), the elastic energy density can be written in divergence form as

$$\begin{aligned} w &= \nabla \cdot \left(\mu \widetilde{\mathbf{E}}\mathbf{u} + \frac{\lambda}{2}(\nabla \cdot \mathbf{u})\mathbf{u} - \overline{\mathbf{T}}\mathbf{u}\right) - \frac{1}{2}\mathbf{u} \cdot (\mu \Delta \mathbf{u} + (\lambda + \mu)\nabla(\nabla \cdot \mathbf{u})) + \alpha_1 \sigma_1 \theta(z) \\ &= \nabla \cdot \left(\mu \widetilde{\mathbf{E}}\mathbf{u} + \frac{\lambda}{2}(\nabla \cdot \mathbf{u})\mathbf{u} - \overline{\mathbf{T}}\mathbf{u}\right) + \alpha_1 \sigma_1 \theta(z) \\ &= \nabla \cdot \left(\frac{1}{2}\widetilde{\mathbf{T}}\mathbf{u} - \overline{\mathbf{T}}\mathbf{u}\right) + \alpha_1 \sigma_1 \theta(z). \end{aligned}$$

Inserting the above divergence form into (9) on a finite subdomain $\Omega_\rho \subseteq \Omega$, the total elastic energy can be written as a boundary integral:

$$W(\mathbf{u}; \Omega_\rho) = \int_{\partial \Omega_\rho} \left(\frac{1}{2}\widetilde{\mathbf{T}}\mathbf{u} - \overline{\mathbf{T}}\mathbf{u}\right) \cdot \mathbf{n}\, dS + \alpha_1 \sigma_1 |\Omega_f \cap \Omega_\rho|,$$

where Ω_f denotes the film. Similarly,

$$W(\mathbf{u}^m; \Omega_\rho^m) = \int_{\partial \Omega_\rho^m} \left(\frac{1}{2}\widetilde{\mathbf{T}}^m\mathbf{u}^m - \overline{\mathbf{T}}\mathbf{u}^m\right) \cdot \mathbf{n}\, dS + \alpha_1 \sigma_1 |\Omega_f^m \cap \Omega_\rho^m|.$$

Recalling (7) and taking the limit as $\rho \to \infty$, (10) gives the exact correction to the energy barrier:

$$\Delta W = \frac{1}{2}\int_{\partial \Omega^m} \mathbf{u}^m \cdot \overline{\mathbf{T}}\mathbf{n}\, dS - \frac{1}{2}\int_{\partial \Omega} \mathbf{u} \cdot \overline{\mathbf{T}}\mathbf{n}\, dS + \alpha_1 \sigma_1 |\Omega \backslash \Omega^m|.$$

Likewise, using (11) and (12), we find the Energy Localization Approximation and Energy Truncation Approximation, respectively, of the correction

to the energy barrier:

$$\begin{aligned}\Delta W_L &= \frac{1}{2}\int_{\Gamma^m} \mathbf{u}_\rho^m \cdot \overline{\mathbf{T}}\mathbf{n}\, dS - \frac{1}{2}\int_{\Gamma} \mathbf{u}\cdot\overline{\mathbf{T}}\mathbf{n}\, dS + \alpha_1\sigma_1|\Omega\backslash\Omega^m| + \\ &\quad \frac{1}{2}\int_{\Gamma_\rho} \mathbf{u}\cdot\left(\widetilde{\mathbf{T}} - \widetilde{\mathbf{T}}_\rho^m\right)\mathbf{n}\, dS, \\ \Delta W_T &= \frac{1}{2}\int_{\Gamma^m} \mathbf{u}^m \cdot \overline{\mathbf{T}}\mathbf{n}\, dS - \frac{1}{2}\int_{\Gamma} \mathbf{u}\cdot\overline{\mathbf{T}}\mathbf{n}\, dS + \alpha_1\sigma_1|\Omega\backslash\Omega^m| + \\ &\quad \frac{1}{2}\int_{\Gamma_\rho} \left(\mathbf{u}\cdot\widetilde{\mathbf{T}} - \mathbf{u}^m\cdot\widetilde{\mathbf{T}}^m\right)\mathbf{n}\, dS + \int_{\Gamma_\rho}(\mathbf{u}^m - \mathbf{u})\cdot\overline{\mathbf{T}}\mathbf{n}\, dS,\end{aligned}$$

where the boundaries $\partial\Omega_\rho = \Gamma\cup\Gamma_\rho$ and $\partial\Omega_\rho^m = \Gamma^m\cup\Gamma_\rho$ have been decomposed into surface and subsurface components (see Figure 1). The corresponding errors of each approximation are then:

$$\begin{aligned}E_L &= \frac{1}{2}\int_{\partial\Omega^m\backslash\Gamma^m} \mathbf{u}^m\cdot\overline{\mathbf{T}}\mathbf{n}\, dS - \frac{1}{2}\int_{\partial\Omega\backslash\Gamma}\mathbf{u}\cdot\overline{\mathbf{T}}\mathbf{n}\, dS \\ &\quad -\frac{1}{2}\int_{\Gamma_\rho}\mathbf{u}\cdot\left(\widetilde{\mathbf{T}} - \widetilde{\mathbf{T}}_\rho^m\right)\mathbf{n}\, dS + \frac{1}{2}\int_{\Gamma^m}(\mathbf{u}^m - \mathbf{u}_\rho^m)\cdot\overline{\mathbf{T}}\mathbf{n}\, dS, \quad (13)\end{aligned}$$

and

$$\begin{aligned}E_T &= \frac{1}{2}\int_{\partial\Omega^m\backslash\Gamma^m} \mathbf{u}^m\cdot\overline{\mathbf{T}}\mathbf{n}\, dS - \frac{1}{2}\int_{\partial\Omega\backslash\Gamma}\mathbf{u}\cdot\overline{\mathbf{T}}\mathbf{n}\, dS \\ &\quad -\frac{1}{2}\int_{\Gamma_\rho}\left(\mathbf{u}\cdot\widetilde{\mathbf{T}} - \mathbf{u}^m\cdot\widetilde{\mathbf{T}}^m\right)\mathbf{n}\, dS - \int_{\Gamma_\rho}(\mathbf{u}^m - \mathbf{u})\cdot\overline{\mathbf{T}}\mathbf{n}\, dS. \quad (14)\end{aligned}$$

2.2.1. Approximate Evaluation of Error Formulas. In order to compare the two approximations, we aim to find asymptotic expressions for the errors given by (13) and (14) in terms of $1/\rho$. As a reminder, we take a film profile $H + h(x, y)$, where $h(x, y) = 0$ for $x^2 + y^2 > R^2$. In addition, we take h, h_x, and h_y to be $O(\epsilon)$ for $x^2 + y^2 < R^2$. We note that the normal along the surface of the film is

$$\mathbf{n} = \frac{(-h_x(x,y), -h_y(x,y), 1)^T}{\sqrt{1 + h_x^2(x,y) + h_y^2(x,y)}} \sim \mathbf{e}_3 - h_x(x,y)\mathbf{e}_1 - h_y(x,y)\mathbf{e}_2.$$

Then, to leading order, $\mathbf{n} \sim \mathbf{e}_3$. Hence, we approximate the film/vacuum interface as flat when applying the boundary conditions given in (7). At this

point, it is convenient to translate the film/substrate medium such that the film/vacuum interface is at $z = 0$. Then, it follows from (3) that

$$\overline{\mathbf{T}} = \begin{pmatrix} \sigma_1 & 0 & 0 \\ 0 & \sigma_1 & 0 \\ 0 & 0 & 0 \end{pmatrix} \theta(z + H). \tag{15}$$

Furthermore, it follows from the boundary condition (7) that

$$\widetilde{\mathbf{T}}\mathbf{e}_3 = -\sigma_1 \left(h_x(x, y)\mathbf{e}_1 + h_y(x, y)\mathbf{e}_2\right) \quad \text{at } z = 0.$$

The resulting problem for the half-space is then

$$\begin{aligned} \mu\Delta\mathbf{u} + (\lambda + \mu)\nabla\left(\nabla \cdot \mathbf{u}\right) &= \mathbf{0} \quad \text{for } z < 0, \\ \widetilde{\mathbf{T}}\mathbf{e}_3 &= -\sigma_1 \left(h_x(x, y)\mathbf{e}_1 + h_y(x, y)\mathbf{e}_2\right) \quad \text{at } z = 0, \\ \mathbf{u} &\to \mathbf{0} \quad \text{as } |\mathbf{x}| \to \infty. \end{aligned} \tag{16}$$

The solution to the above half-space problem can be obtained by following the derivation by Landau and Lifshitz [5]:

$$\mathbf{u} = -\sigma_1 \int \int_{x'^2 + y'^2 \le R^2} \mathbf{f}(x - x', y - y', z) h(x', y') \, dx'dy' \tag{17}$$

where

$$\mathbf{f} = \frac{1}{4\pi\mu} \begin{bmatrix} \frac{x}{r^3}\left(\frac{\lambda+2\mu}{\lambda+\mu} - \frac{3z^2}{r^2}\right) \\ \frac{y}{r^3}\left(\frac{\lambda+2\mu}{\lambda+\mu} - \frac{3z^2}{r^2}\right) \\ \frac{z}{r^3}\left(\frac{\lambda}{\lambda+\mu} - \frac{3z^2}{r^2}\right) \end{bmatrix} = \frac{\partial}{\partial x}\mathbf{G}\mathbf{e}_1 + \frac{\partial}{\partial y}\mathbf{G}\mathbf{e}_2,$$

$\mathbf{G}$ is the Green's tensor for

$$\begin{aligned} \mu\Delta\mathbf{u} + (\lambda + \mu)\nabla\left(\nabla \cdot \mathbf{u}\right) &= \mathbf{0} \quad \text{for } z < 0, \\ \widetilde{\mathbf{T}}\mathbf{e}_3 &= -\sigma_1 (h_x(x, y)\delta(x, y)\mathbf{e}_1 + h_y(x, y)\delta(x, y)\mathbf{e}_2) \quad \text{at } z = 0, \\ \mathbf{u} &\to \mathbf{0} \quad \text{as } |\mathbf{x}| \to \infty, \end{aligned}$$

and $r = \sqrt{x^2 + y^2 + z^2}$. Similarly, we obtain $\mathbf{u}^m$ with $h(x, y)$ replaced by $h^m(x, y)$.

At this point, we aim to derive asymptotic expressions for each of the integrals appearing in (13) and (14). Namely, we show that

$$I_1 = \frac{1}{2}\int_{\partial\Omega^m\setminus\Gamma^m} \mathbf{u}^m \cdot \overline{\mathbf{T}}\mathbf{n}\, dS = 0,$$

$$I_2 = \frac{1}{2}\int_{\partial\Omega\setminus\Gamma} \mathbf{u} \cdot \overline{\mathbf{T}}\mathbf{n}\, dS = 0,$$

$$I_3 = \frac{1}{2}\int_{\Gamma_\rho} (\mathbf{u}\cdot\widetilde{\mathbf{T}} - \mathbf{u}^m\cdot\widetilde{\mathbf{T}}^m)\mathbf{n}\, dS = O(\epsilon^2/\rho^3), \tag{18}$$

$$I_4 = \int_{\Gamma_\rho} (\mathbf{u}^m - \mathbf{u})\cdot\overline{\mathbf{T}}\mathbf{n}\, dS = O(\epsilon H/\rho), \tag{19}$$

$$I_5 = \frac{1}{2}\int_{\Gamma_\rho} \mathbf{u}\cdot(\widetilde{\mathbf{T}} - \widetilde{\mathbf{T}}^m_\rho)\mathbf{n}\, dS = O(\epsilon^2/\rho^3). \tag{20}$$

and

$$I_6 = \frac{1}{2}\int_{\Gamma^m} (\mathbf{u}^m - \mathbf{u}^m_\rho)\cdot\overline{\mathbf{T}}\mathbf{n}\, dS = O(\epsilon/\rho^3), \tag{21}$$

We recall that the film/vacuum interface is flat for $|\mathbf{x}| > R$. Hence, for $\rho > R$, $I_1 = I_2 = 0$ since $\overline{\mathbf{T}}\mathbf{n} = \mathbf{0}$ (owing to $\sigma_2 = 0$). Using this fact, and equations (18) and (19), we establish Theorem 2:

$$E_T = O(\epsilon H/\rho).$$

It follows from equations (20) and (21) that

$$E_L = O(\epsilon/\rho^3),$$

which establishes Theorem 1.

2.2.2. Derivation of Error Estimates. In this section, we establish the estimates provided in the previous section.

Proof of Eq. 18. Recall that

$$I_3 = \frac{1}{2}\int_{\Gamma_\rho} (\mathbf{u}\cdot\widetilde{\mathbf{T}} - \mathbf{u}^m\cdot\widetilde{\mathbf{T}}^m)\mathbf{n}\, dS.$$

Furthermore, we recall (17) and its analogue

$$\mathbf{u}^m = -\sigma_1 \int \int_{x'^2+y'^2 \le R^2} \mathbf{f}(x-x', y-y', z) h^m(x', y')\ dx'dy'.$$

We need to evaluate $\mathbf{u}$ and $\widetilde{\mathbf{T}}$ on the lower hemisphere of radius ρ centered at $\mathbf{x} = (0,0,0)$. We begin by converting each of the integrals to polar coordinates:

$$\mathbf{u} = -\sigma_1 \int_0^{2\pi} \int_0^R \mathbf{f}(x - s\cos\beta, y - s\sin\beta, z) h(s\cos\beta, s\sin\beta) s\ dsd\beta$$

and

$$\mathbf{u}^m = -\sigma_1 \int_0^{2\pi} \int_0^R \mathbf{f}(x - s\cos\beta, y - s\sin\beta, z) h^m(s\cos\beta, s\sin\beta) s\ dsd\beta.$$

Let $(x,y,z) = \rho(\sin\varphi\cos\theta, \sin\varphi\sin\theta, \cos\varphi)$ and substitute this into the integrals above. Then, by writing the integrand as a Taylor series in s and expanding in terms of $1/\rho$, we obtain

$$\mathbf{u}\,\big|_{|\mathbf{x}|=\rho} = O(\epsilon/\rho^2) \quad \text{and} \quad \mathbf{u}^m\,\big|_{|\mathbf{x}|=\rho} = O(\epsilon/\rho^2), \tag{22}$$

where we have used the fact that $h(x,y) = O(\epsilon)$. Similarly, we obtain

$$\widetilde{\mathbf{T}}\,\big|_{|\mathbf{x}|=\rho} = O(\epsilon/\rho^3) \quad \text{and} \quad \widetilde{\mathbf{T}}^m\,\big|_{|\mathbf{x}|=\rho} = O(\epsilon/\rho^3). \tag{23}$$

Since the area of Γ_ρ is proportional to ρ^2, combining (22) and (23) in the expression for I_3 yields (18).

Proof of Eq. 19. Recall that

$$I_4 = \int_{\Gamma_\rho} (\mathbf{u}^m - \mathbf{u}) \cdot \overline{\mathbf{T}}\mathbf{n}\, dS.$$

We note that $\overline{\mathbf{T}}\mathbf{n} = \mathbf{0}$ in the substrate. So, the only contribution to I_4 is when Γ_ρ coincides with the film. Furthermore, for $\rho \gg H$, the area of Γ_ρ coinciding with the film is proportional to ρH. Combining this with (22) yields (19).

Proof of Eq. 20. Recall that

$$I_5 = \frac{1}{2} \int_{\Gamma_\rho} \mathbf{u} \cdot (\widetilde{\mathbf{T}} - \widetilde{\mathbf{T}}^m_\rho)\mathbf{n}\, dS.$$

Let $\mathbf{v} = \mathbf{u} - \mathbf{u}_\rho^m$. Then, the integral can be rewritten as

$$\frac{1}{2}\int_{\Gamma_\rho} \mathbf{u}\cdot(\widehat{\mathbf{T}}\mathbf{v})\mathbf{n}\,dS, \tag{24}$$

where the operator $\widehat{\mathbf{T}}$ is defined through

$$(\widehat{T}v)_{ij} = \mu(\partial_i v_j + \partial_j v_i) + \lambda\delta_{ij}\partial_k v_k.$$

We now need to estimate $\widehat{\mathbf{T}}\mathbf{v}$. We note that $\mathbf{v}$ satisfies the system

$$\begin{aligned}
\mu\Delta\mathbf{v} + (\lambda+\mu)\nabla(\nabla\cdot\mathbf{v}) &= 0 \quad \text{for } z<0 \text{ and } |\mathbf{x}|<\rho,\\
(\widehat{\mathbf{T}}\mathbf{v})\mathbf{e}_3 &= -\sigma_1(\widetilde{h}_x(x,y)\mathbf{e}_1 + \widetilde{h}_y(x,y)\mathbf{e}_2) \quad \text{at } z=0 \text{ and } x^2+y^2<\rho^2,\\
\mathbf{v} &= 0 \quad \text{for } z<0 \text{ and } |\mathbf{x}|=\rho.
\end{aligned} \tag{25}$$

Let $\mathbf{x} = \rho\mathbf{x}'$, $\mathbf{v}' = \mathbf{v}(\rho\mathbf{x}')$ and $\widetilde{h}'(x',y') = \widetilde{h}(\rho x', \rho y')$. Then, the system given by (25) can be transformed into the following system:

$$\begin{aligned}
\mu\Delta'\mathbf{v}' + (\lambda+\mu)\nabla'(\nabla'\cdot\mathbf{v}') &= 0 \quad \text{for } z'<0 \text{ and } |\mathbf{x}'|<1,\\
(\widehat{\mathbf{T}}'\mathbf{v}')\mathbf{e}_3 &= -\sigma_1(\widetilde{h}'_{x'}(x',y')\mathbf{e}_1 + \widetilde{h}'_{y'}(x',y')\mathbf{e}_2) \quad \text{at } z'=0 \text{ and } x'^2+y'^2<1,\\
\mathbf{v}' &= 0 \quad \text{for } z'<0 \text{ and } |\mathbf{x}'|=1.
\end{aligned} \tag{26}$$

For $\rho > R$, the solution to this problem can be written as

$$\mathbf{v}' = -\sigma_1\int\int_{s^2+t^2\le(R/\rho)^2} \mathbf{f}_1(x'-s, y'-t, z')\widetilde{h}'(s,t)\,dsdt,$$

where

$$\mathbf{f}_1 = \frac{\partial}{\partial x}\mathbf{G}_1\mathbf{e}_1 + \frac{\partial}{\partial y}\mathbf{G}_1\mathbf{e}_2,$$

$\mathbf{G}_1$ is the Green's tensor for (26), and we have used the fact that $\widetilde{h}$ is supported on the disc of radius R.

Since

$$\widehat{\mathbf{T}}\mathbf{v} = \rho^{-1}\,\widehat{\mathbf{T}}'\mathbf{v}',$$

we have

$$\widehat{\mathbf{T}}\mathbf{v} = -\frac{\sigma_1}{\rho}\int\int_{s^2+t^2\le(R/\rho)^2} \widehat{\mathbf{T}}'\mathbf{f}_1(x'-s, y'-t, z)\widetilde{h}'(s,t)\,dsdt = O(\epsilon/\rho^3).$$

We note that $\widehat{\mathbf{T}}'\mathbf{f}_1(x'-s,y'-t,z) = O(1)$ and $\widetilde{h}'(s,t) = O(\epsilon)$. Hence, the integrand is $O(\epsilon)$. Combining this with (22) and (24) gives (20).

Proof of Eq. 21. Recall that

$$I_6 = \frac{1}{2}\int_{\Gamma^m} (\mathbf{u}^m - \mathbf{u}^m_\rho)\cdot\overline{\mathbf{T}}\mathbf{n}\, dS.$$

For $\rho > R$, we can use (15) and the leading order approximation of the normal to rewrite I_6 as

$$I_6 = \frac{\sigma_1}{2}\int\int_{x^2+y^2\le R^2} (\mathbf{u}^m_\rho(x,y,0) - \mathbf{u}^m(x,y,0))\cdot(h^m_x(x,y)\mathbf{e}_1 + h^m_y(x,y)\mathbf{e}_2)\, dxdy. \tag{27}$$

Let $\mathbf{w} = \mathbf{u}^m_\rho - \mathbf{u}^m$, $\widetilde{\mathbf{u}} = \mathbf{u} - \mathbf{u}^m$ and $\widetilde{h} = h - h^m$. We recall that $\mathbf{u}^m_\rho(|\mathbf{x}| = \rho) = \mathbf{u}(|\mathbf{x}| = \rho)$. Then, since $\mathbf{u}^m_\rho$ and $\mathbf{u}^m$ satisfy the first two equations of (16) on Ω_ρ, with h replaced by h^m, $\mathbf{w}$ satisfies the following system:

$$\begin{aligned} \mu\Delta\mathbf{w} + (\lambda+\mu)\nabla(\nabla\cdot\mathbf{w}) &= 0 \quad \text{for } z<0 \text{ and } |\mathbf{x}|<\rho, \\ (\widehat{\mathbf{T}}\mathbf{w})\mathbf{e}_3 &= 0 \quad \text{at } z=0 \text{ and } |\mathbf{x}|\le\rho, \\ \mathbf{w} &= \widetilde{\mathbf{u}} \quad \text{at } z<0 \text{ and } |\mathbf{x}|=\rho. \end{aligned} \tag{28}$$

We note that $\widetilde{\mathbf{u}}$ satisfies (16) with h replaced by $\widetilde{h}$. Then, appealing to (17), we find

$$\widetilde{\mathbf{u}} = -\sigma_1\int\int_{x'^2+y'^2\le R^2} \mathbf{f}(x-x',y-y',z)\widetilde{h}(x',y')\, dx'dy'.$$

We need to evaluate $\widetilde{\mathbf{u}}$ on the lower hemisphere of radius ρ centered at $(0,0,0)$. We begin by converting the above integral to polar coordinates:

$$\widetilde{\mathbf{u}} = -\sigma_1\int_0^{2\pi}\int_0^R \mathbf{f}(x-s\cos\beta, y-s\sin\beta, z)\widetilde{h}(s\cos\beta, s\sin\beta)s\, dsd\beta.$$

Then,

$$\begin{aligned} \widetilde{\mathbf{u}}\big|_{|\mathbf{x}|=\rho} = &-\sigma_1\int_0^{2\pi}\sum_{n=0}^{\infty}\frac{a_n(\beta)\left(\sum_{i=0}^{\lceil\frac{n+1}{2}\rceil-1}\left(\sum_{j=0}^{n-2i}\binom{n-2i}{j}(\cos\beta)^j(\sin\beta)^{n-2i-j}\mathbf{b}_{nij}(\varphi,\theta)\right)\right)}{\rho^{n+2}}\, d\beta \\ &-\sigma_1\int_0^{2\pi}\sum_{n=0}^{\infty}\frac{a_n(\beta)\left(\sum_{i=0}^{\lceil\frac{n}{2}\rceil-1}\left(\sum_{j=0}^{n-1-2i}\binom{n-1-2i}{j}(\cos\beta)^j(\sin\beta)^{n-1-2i-j}\left(\cos\beta\mathbf{c}_{nij}(\varphi,\theta)+\sin\beta\mathbf{d}_{nij}(\varphi,\theta)\right)\right)\right)}{\rho^{n+2}}\, d\beta \end{aligned}$$

where $a_n(\beta) = \int_0^R \widetilde{h}(s\cos\beta, s\sin\beta)s^{n+1}\,ds$,

$$\mathbf{b}_{nij}(\varphi,\theta) = \frac{(-1)^{i+1}\prod_{k=0}^{2i-1}(n-k)}{4\pi n!\mu(\lambda+\mu)}\begin{bmatrix} \frac{(\cos\theta)^{j+1}(\sin\theta)^{n-2i-j}(\sin\varphi)^{n+1-2i}}{2^i\cdot i!}\cdot \\ \left((\lambda+\mu)(\cos\varphi)^2\prod_{k=0}^{n+1-i}(1+2k) - (\lambda+2\mu)\prod_{k=0}^{n-i}(1+2k)\right) \\ \\ \frac{(\cos\theta)^{j}(\sin\theta)^{n-2i-j+1}(\sin\varphi)^{n+1-2i}}{2^i\cdot i!}\cdot \\ \left((\lambda+\mu)(\cos\varphi)^2\prod_{k=0}^{n+1-i}(1+2k) - (\lambda+2\mu)\prod_{k=0}^{n-i}(1+2k)\right) \\ \\ \frac{(\cos\theta)^{j}(\sin\theta)^{n-2i-j}(\sin\varphi)^{n-2i}\cos\varphi}{2^i\cdot i!}\cdot \\ \left((\lambda+\mu)(\cos\varphi)^2\prod_{k=0}^{n+1-i}(1+2k) - \lambda\prod_{k=0}^{n-i}(1+2k)\right) \end{bmatrix}$$

for $n \in [0,\infty)$, $i \in [0, \lceil\frac{n+1}{2}\rceil - 1]$ and $j \in [0, n-2i]$,

$$\mathbf{c}_{nij}(\varphi,\theta) = \frac{(-1)^{i}\prod_{k=0}^{2i-1}(n-1-k)}{4\pi(n-1)!\mu(\lambda+\mu)}\begin{bmatrix} \frac{(\cos\theta)^{j}(\sin\theta)^{n-1-2i-j}(\sin\varphi)^{n-1-2i}}{2^i\cdot i!}\cdot \\ \left((\lambda+\mu)(\cos\varphi)^2\prod_{k=0}^{n-i}(1+2k) - \lambda\prod_{k=0}^{n-1-i}(1+2k)\right) \\ \\ 0 \\ \\ 0 \end{bmatrix}$$

for $n \in [0,\infty)$, $i \in [0, \lceil\frac{n}{2}\rceil - 1]$ and $j \in [0, n-1-2i]$,

$$\mathbf{d}_{nij}(\varphi,\theta) = \frac{(-1)^{i}\prod_{k=0}^{2i-1}(n-1-k)}{4\pi(n-1)!\mu(\lambda+\mu)}\begin{bmatrix} 0 \\ \\ \frac{(\cos\theta)^{j}(\sin\theta)^{n-1-2i-j}(\sin\varphi)^{n-1-2i}}{2^i\cdot i!}\cdot \\ \left((\lambda+\mu)(\cos\varphi)^2\prod_{k=0}^{n-i}(1+2k) - \lambda\prod_{k=0}^{n-1-i}(1+2k)\right) \\ \\ 0 \end{bmatrix}$$

for $n \in [0,\infty)$, $i \in [0, \lceil\frac{n}{2}\rceil - 1]$ and $j \in [0, n-1-2i]$.

We can now write the solution of (28) as

$$\begin{aligned}\mathbf{w} = &-\sigma_1\int_0^{2\pi}\sum_{n=0}^{\infty}\frac{a_n(\beta)\left(\sum_{i=0}^{\lceil\frac{n+1}{2}\rceil-1}\left(\sum_{j=0}^{n-2i}\binom{n-2i}{j}(\cos\beta)^j(\sin\beta)^{n-2i-j}\mathbf{w}^1_{nij}\left(\frac{|\mathbf{x}|}{\rho}\right)\right)\right)}{\rho^{n+2}}\,d\beta \\ &-\sigma_1\int_0^{2\pi}\sum_{n=0}^{\infty}\frac{a_n(\beta)\left(\sum_{i=0}^{\lceil\frac{n}{2}\rceil-1}\left(\sum_{j=0}^{n-1-2i}\binom{n-1-2i}{j}(\cos\beta)^j(\sin\beta)^{n-1-2i-j}\left(\cos\beta\mathbf{w}^2_{nij}\left(\frac{|\mathbf{x}|}{\rho}\right)+\sin\beta\mathbf{w}^3_{nij}\left(\frac{|\mathbf{x}|}{\rho}\right)\right)\right)\right)}{\rho^{n+2}}\,d\beta,\end{aligned} \tag{29}$$

where $\mathbf{w}^k_{nij}$ satisfies (28) except that the subsurface boundary condition is

replaced by

$$\mathbf{w}_{nij}^{k} = \begin{cases} \mathbf{b}_{nij} & \text{if } k = 1 \\ \mathbf{c}_{nij} & \text{if } k = 2 \\ \mathbf{d}_{nij} & \text{if } k = 3 \end{cases} \qquad \text{for} \quad |\mathbf{x}| = 1 \text{ and } z < 0.$$

We note that for $n = 0$, the only term is $\mathbf{b}_{000}$. Since $\mathbf{b}_{000} \cdot \mathbf{e}_1$ is antisymmetric about $\theta = \pi/2$ and $\mathbf{b}_{000} \cdot \mathbf{e}_2$ is antisymmetric about $\theta = 0$, we infer that $\mathbf{e}_1 \cdot \mathbf{w}_{000}^1(0,0,0) = 0$ and $\mathbf{e}_2 \cdot \mathbf{w}_{000}^1(0,0,0) = 0$. It follows then from (29) that

$$\mathbf{e}_1 \cdot \mathbf{w}(0,0,0) = O(1/\rho^3)$$

and

$$\mathbf{e}_2 \cdot \mathbf{w}(0,0,0) = O(1/\rho^3).$$

Furthermore, differentiating (29), we find that

$$\partial_x((\mathbf{e}_1 + \mathbf{e}_2) \cdot \mathbf{w})(0,0,0) = O(1/\rho^3)$$

and

$$\partial_y((\mathbf{e}_1 + \mathbf{e}_2) \cdot \mathbf{w})(0,0,0) = O(1/\rho^3).$$

Therefore, we conclude that

$$(\mathbf{e}_1 + \mathbf{e}_2) \cdot \mathbf{w}(x,y,0) = O(1/\rho^3) \quad \text{provided} \quad x^2 + y^2 = O(1).$$

Substituting this last result into (27) and using the fact that both $h_x = O(\epsilon)$ and $h_y = O(\epsilon)$, we obtain (21).

3. Summary. A common issue one must deal with in the simulation of heteroepitaxial growth using KMC is the long range nature of the elastic interactions. Schulze and Smereka previously considered a local approximation technique that was observed to yield highly accurate approximations of the energy barrier for adatom diffusion in numerical computations on a two-dimensional lattice. Using a continuum analogue of the discrete model, they were able to explain these results and derive estimates for the error as a function of the size of the local region.

In this current work, we have extended those previous results to a three-dimensional lattice. As one may expect, we have shown that the error scales by a factor of one over the size of the box in the localized approximation

when transitioning from a two-dimensional to a three-dimensional lattice. By comparing this result to a more intuitive Energy Truncation Approximation, we have further demonstrated the high accuracy of the Energy Localization Approximation and its utility in KMC simulations of heteroepitaxial growth.

4. Acknowledgments. This work was supported by NSF FRG grant DMS 0854870. We thank Peter Smereka for several helpful conversations.

REFERENCES

[1] R. J. Asaro and W.A. Tiller, *Interface morphology development during stress corrosion cracking: Part I. Via surface diffusion*, Metallurgical Transactions, 3(1972), pp. 1789-1796.

[2] J. E. Ayers, *Heteroepitaxy of Semiconductors: Theory, Growth, and Characterization*, CRC Press, Boca Raton, FL, 2007.

[3] P. Fratzl, J. L. Lebowitz, and O. Penrose, *Modeling of Phase Separation in Alloys with Coherent Elastic Misfit*, J. Stat. Phys., 95(1999), pp. 1429-1503.

[4] M. A. Grinfeld, *instability of interface between nonhydrostatically stressed elastic body and melts*, Doklady Akademii Nauk SSSR, 290(1986), pp. 1358-1363.

[5] L. D. Landau and E. M. Lifshitz, *Theory of Elasticity Third ed*, Pergamon Press, Oxford, England, 1986.

[6] C. H. Lam, C. K. Lee, and L. M. Sander, *Competing Roughening Mechanisms in Strained Heteroepitaxy: A Fast Kinetic Monte Carlo Study*, Phys. Rev. Lett., 89(2002), 216102 (1-4).

[7] M. T. Lung, C. H. Lam, and L. M. Sander, *Island, pit, and groove formation in strained heteroepitaxy*, Phys. Rev. Lett., 95(2005), 086102 (1-4).

[8] G. Russo and P. Smereka, *Computation of Strained Epitaxial Growth in Three Dimensions by Kinetic Monte Carlo*, J. Comput. Phys., 214(2005), pp. 809-828.

[9] T. P. Schulze and P. Smereka, *An Energy Localization Principle and its Application to Fast Kinetic Monte Carlo Simulation of Heteroepitaxial Growth*, J. Mech. Phys. Solids, 57(2009), pp. 521 - 538.

[10] T.P. Schulze and P. Smereka, *Simulation of Three-Dimensional Strained Heteroepitaxial Growth using Kinetic Monte Carlo*, Commun. Comput. Phys., 10 (#5)(2011), pp. 1089-1112.

[11] T.P. Schulze and P. Smereka, *Kinetic Monte Carlo Simulation of Heteroepitaxial Growth: Wetting Layers, Quantum Dots, Capping, and NanoRings*, Phys. Rev. B, 86(2012), 235313.